Pramana – J. Phys. (2020) 94:47
https://doi.org/10.1007/s12043-020-1915-z

Models for membrane curvature sensing of curvature generating proteins

T V SACHIN KRISHNAN[1],*, SOVAN L DAS[2] and P B SUNIL KUMAR[1,3]

[1]Department of Physics, Indian Institute of Technology Madras, Chennai 600 036, India
[2]Department of Mechanical Engineering, Indian Institute of Technology Palakkad, Palakkad 678 557, India
[3]Department of Physics, Indian Institute of Technology Palakkad, Palakkad 678 557, India
*Corresponding author. E-mail: sachin@physics.iitm.ac.in

MS received 16 July 2019; revised 9 October 2019; accepted 12 December 2019

Abstract. The curvature-sensitive localisation of proteins on membranes is vital for many cell biological processes. Coarse-grained models are routinely employed to study the curvature-sensing phenomena and membrane morphology at the length scale of a few micrometres. Two prevalent phenomenological models exist for modelling the experimental observations of curvature sensing: (1) the spontaneous curvature (SC) model and (2) the curvature mismatch (CM) model, which differ in their treatment of the change in elastic energy due to the binding of proteins on the membrane. In this work, the prediction of sensing and generation behaviour by these two models are investigated using analytical calculations as well as dynamic triangulation Monte Carlo simulations of quasispherical vesicles. While the SC model yields a monotonically decreasing sensing curve as a function of the vesicle radius, the CM model results in a non-monotonic sensing curve. We highlight the main differences in the interpretation of the protein-related parameters in the two models. We further propose that the SC model is appropriate for modelling peripheral proteins employing the hydrophobic insertion mechanism, with minimal modification of membrane rigidity, while the CM model is appropriate for modelling curvature generation using scaffolding mechanism where there is significant stiffening of the membrane due to protein binding.

Keywords. Biological membranes; curvature sensing; curvature generation.

PACS Nos **87.16.D–; 87.14.E–**

1. Introduction

Protein-mediated regulation of membrane curvature occurs during many cellular processes such as cargo trafficking, cell motility, cell growth and division [1–4]. Recently, several classes of proteins capable of curvature generation have been identified [5–7]. Dynamin and proteins with the crescent-shaped Bin Amphiphysin Rvs (BAR) domain were found to generate curvature by the scaffolding mechanism [8]. On the other hand, epsin protein with an N-terminal helix generates curvature using the hydrophobic insertion mechanism [9,10]. These curvature-generating proteins are also capable of sensing membrane curvature [11]. Curvature sensing refers to the ability of proteins to bind onto the membranes depending on the local curvature. Recent experiments have reported that membrane curvature gives a cue to the localisation of proteins in bacteria and viruses [12–15]. This phenomenon is believed to be exploited by cells during the process of budding and fission. For example, in the clathrin-mediated membrane fission, the narrow neck between the clathrin-bound bud and the parent membrane preferentially recruits the dynamin proteins responsible for membrane scission. Thus, it is important to understand these processes of curvature sensing and generation to gain insight into many of the cellular processes.

Biophysical experimental set-ups such as single liposome curvature (SLiC) assays and tethers pulled from giant unilamellar vesicles (GUVs) have been extensively used to quantify curvature sensing [16,17]. These two methods are schematically illustrated in figure 1. Considering their small throughput, *in vivo* alternatives have also been used [18]. In the tether pulling experiments, a narrow membrane tube of a few tens of nanometre radius is pulled from a GUV of a few microns radius. Curvature-sensitive proteins are introduced to these two-membrane surfaces with very

Published online: 25 February 2020

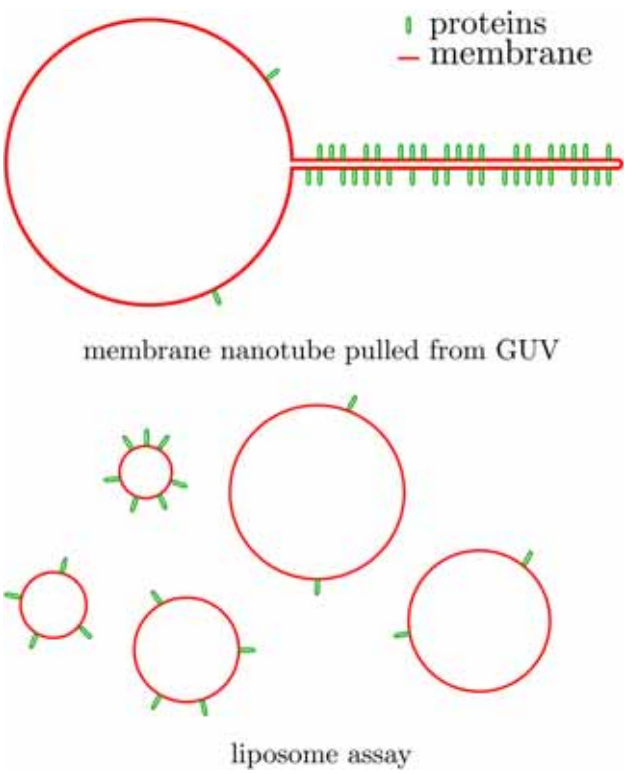

Figure 1. Schematic of preferential binding of proteins to highly curved membrane surfaces. Typical biophysical experimental set-ups used to study curvature sensing phenomena: membrane nanotube pulled from GUV (top) and liposome assay (bottom).

different curvatures. The relative binding fraction of proteins on the two surfaces is then measured based on the intensity of fluorescently tagged proteins. On the other hand, in SLiC assays, proteins are introduced in a medium containing liposomes of different radii [9]. Similar to the case of tether pulling experiments, the intensity of fluorescently tagged proteins is utilised to estimate the binding fraction of proteins on liposome surfaces.

Several quantitative analytical models have also been proposed to study the phenomena of curvature sensing [19–21]. Currently, there exist two thermodynamic models for curvature sensing/generation – the spontaneous curvature (SC) model and the curvature mismatch (CM) model. The two models differ in their treatment of the membrane elastic energy due to the deformation induced by proteins. Although both the models have been shown to fit various experimental data, it is not clear which among the two models is more suitable to study the curvature sensing/generation behaviour of a particular protein. In the present work, we describe the two models and compare the results obtained using analytical calculations as well as Monte Carlo (MC) simulations.

The article is organised as follows: Section 2 introduces the two thermodynamic models and presents analytical results. In §3, we discuss the sensing/generation behaviour of the two models studied using MC simulations. The article ends with a few concluding remarks in §4.

2. Models for curvature sensing

The curvature-sensing ability of proteins is a consequence of the interaction between the proteins and the membrane. Although the specific interactions between membrane patches and protein domains are quite complicated, their effects can be understood in terms of a few coarse-grained interaction parameters. At mesoscopic length scales, several quantitative analytical models have been proposed to study the phenomena of curvature sensing. Below we describe and compare two models, which are most often used.

2.1 *SC model*

SC model assumes that the only effect of the bound protein, on the elastic energy, is to induce a preferred local curvature of the membrane. This model has been employed previously to study sorting of amphiphysin in tube pulling assays [22] as well as in modelling of lipopolysaccharide-binding on synthetic lipid vesicles [23]. In this model, the energy of the membrane surface is given by the spontaneous curvature form of the Helfrich free energy [24],

$$\mathcal{H} = \int \mathrm{d}A \frac{\kappa}{2} (2H - C_0)^2 , \tag{1}$$

where κ is the bending rigidity and C_0 is the spontaneous curvature of the membrane. The integral is over the entire area of the membrane surface. The spontaneous curvature is usually assumed to be linearly dependent on the protein area fraction ϕ [25,26],

$$C_0 = C_\mathrm{p}\phi, \tag{2}$$

where C_p is the intrinsic curvature of the protein. In essence, this model assumes that the protein sets a preferred local curvature on the membrane depending on its bound density.

We consider the vesicle as a triangulated surface with N_v vertices. A discretised Hamiltonian for this surface can be written as

$$\mathcal{H}_\mathrm{SC} = \frac{\kappa}{2} \sum_{i=1}^{N_\mathrm{v}} (2H_i - C_\mathrm{p}\phi_i)^2 A_i - \mu \sum_{i=1}^{N_\mathrm{v}} \phi_i , \tag{3}$$

where H_i and ϕ_i are respectively the mean curvature and the protein-bound state at vertex i. The concentration of proteins in bulk is taken into account indirectly through the binding affinity parameter μ. The parameter μ is the free energy of the proteins in the reservoir for binding onto the membrane surface. It depends on the interaction energy between the membrane and the protein and also the concentration of the protein in the bulk (c_{bulk}) through the relation

$$\mu = \mu_0 + \log \frac{c_{\text{bulk}}}{c_0}, \tag{4}$$

where μ_0 and c_0 are, respectively, the standard state protein chemical potential and concentration [27].

For small bound fractions, the proteins do not significantly affect the membrane curvature if they are homogeneously distributed over the surface. Therefore, we can simplify the expression for free energy by assuming a perfectly spherical surface with each vertex having the same curvature ($2H$). For such a uniformly spherical surface, the mean curvature at each vertex is simply the inverse of the vesicle radius, i.e. $H_i = H = 1/R$. The variable ϕ_i takes the value 1 in vertices with a bound protein and 0 in others. In this model, protein-bound vertices will have minimum energy when the local curvature matches with intrinsic curvature of the protein. Further, if the area at each vertex A_i is the same, say a, we can write the effective free energy per vertex as a function of the protein-bound fraction $\rho = N_{\text{p}}/N_{\text{v}}$ as

$$f_{\text{SC}}(\rho) = \frac{\kappa a}{2}[(2H)^2(1-\rho) + (2H - C_{\text{p}})^2\rho] - \mu\rho + k_{\text{B}}T\left[\rho\log(\rho) + (1-\rho)\log(1-\rho)\right], \tag{5}$$

where $N_{\text{p}} = \sum_{i=1}^{N_{\text{v}}} \phi_i$ is the total number of vertices occupied by the protein field. The first term is obtained as a result of separating the sums for vertices with and without proteins in eq. (3). The last term in eq. (5) represents the mixing free energy of proteins on the discretised surface. Note that such a mixing free energy is due to the exclusion interaction of proteins on the discretised surface. The protein-bound fraction in equilibrium is obtained by minimising the effective free energy with respect to ρ as

$$\rho_{\text{eq}} = \frac{1}{1 + \mathrm{e}^{-\beta[\mu - \frac{\kappa a C_{\text{p}}}{2}(C_{\text{p}} - 4H)]}}. \tag{6}$$

When $C_{\text{p}} = 0$, the above equation takes the form of the standard Langmuir isotherm. For non-zero C_{p} values, the Langmuir isotherm is recovered by defining the effective chemical potential

$$\mu' = \mu - \frac{\kappa a C_{\text{p}}}{2}(C_{\text{p}} - 4H). \tag{7}$$

The adsorption isotherms for different C_{p} values for the SC model is shown in figure 2a. The isotherms for non-zero spontaneous curvatures are shifted to Langmuir isotherms as predicted by eq. (6). Experiments have reported that the adsorption of some proteins on vesicles follows the Langmuir isotherm [9]. The preferential binding of proteins to vesicles of various sizes is characterised using a curvature-sensing curve, wherein the bound fraction of protein is plotted against the vesicle size at a particular binding affinity. The curvature-sensing curve at $\mu = -4$ is shown in figure 2b. When $C_{\text{p}} = 0$, the protein-bound fraction does not depend on the vesicle radius as there is no coupling between the mean curvature (H) and the protein-bound fraction (ϕ) in eq. (1). Therefore, within the SC model, $C_{\text{p}} = 0$ corresponds to the case where membrane curvature is insensitive to that of protein. For non-zero C_{p}, the bound fraction increases with decreasing vesicle radius, approaching the maximum of 1 as $R \to 0$ (or $H \to \infty$ in eq. (6)). Note that, in the SC model, the protein-bound fraction monotonically decreases with increasing vesicle size.

2.2 *CM model*

CM (CM) model supposes (a) an energy penalty when there is a difference in the local membrane and protein curvatures and (b) curvature stiffness of the membrane to depend on the local protein concentration. It has successfully reproduced the preferential binding of I-BAR proteins to negatively curved membranes [28], sorting of potassium channel KvAP [20], and sorting of transmembrane proteins in live cell filopodia [18]. In the CM model, the Hamiltonian is of the form

$$\mathcal{H} = \int \mathrm{d}A \left[\frac{\kappa}{2}(2H)^2 + \frac{\bar{\kappa}}{2}(2H - C_{\text{p}})^2\phi\right]. \tag{8}$$

Here the first term is the Helfrich energy for the membrane surface and the second term is the CM energy. The parameter $\bar{\kappa}$ decides the strength of the mismatch penalty. In regions where there are no bound proteins, $\phi = 0$, only the first term in eq. (8) contributes to the energy. In this limit of no bound protein, both the SC model and the CM model have the same Hamiltonian.

In order to compare the CM model with the SC model discussed previously, we derive the equilibrium protein-bound fraction on a non-deformable vesicle. The discretised form of the CM free energy model is given by

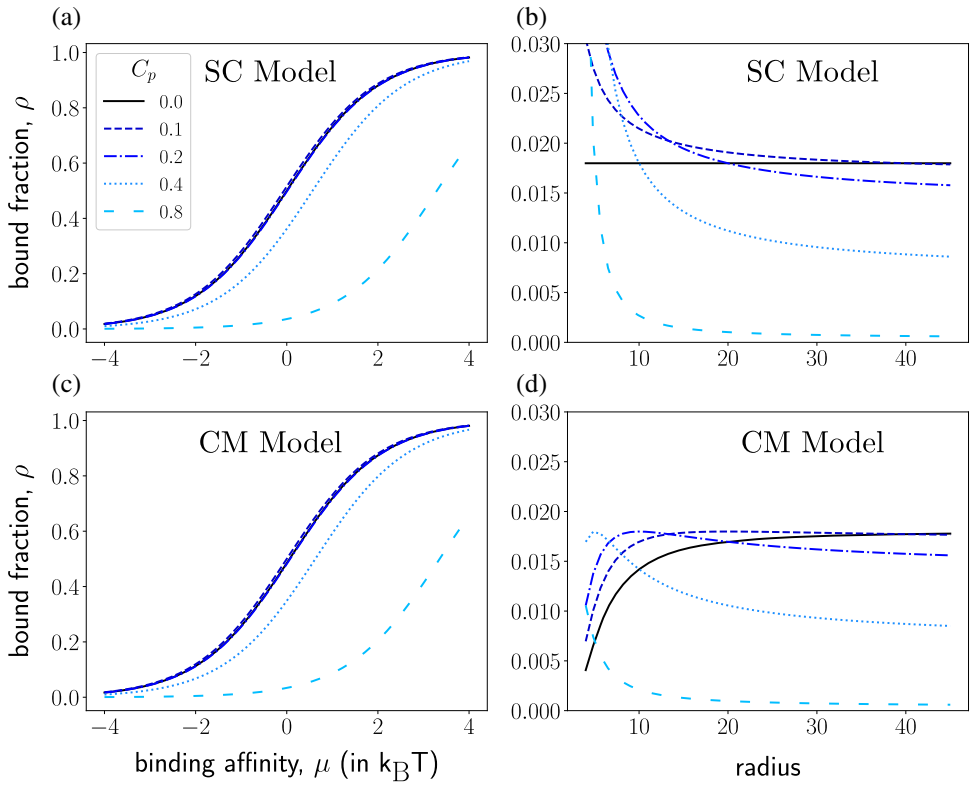

Figure 2. Protein binding on a non-deformable spherical vesicle studied using the SC model and the CM model. Adsorption isotherms of proteins with different C_p values on vesicle of size $R = 21$ in (**a**) the SC model and (**c**) the CM model. Curvature-sensing curves for proteins of various C_p values at $\mu = -4$ for (**b**) the SC model and (**d**) the CM model.

$$\mathcal{H}_{CM} = \sum_{i=1}^{N_v} \left[\frac{\kappa}{2}(2H_i)^2 + \frac{\bar{\kappa}}{2}(2H_i - C_p)^2 \phi_i \right] A_i - \mu \sum_{i=1}^{N_v} \phi_i . \tag{9}$$

In this model, protein-bound vertices will have the same energy as that for the unbound vertices, when the local curvature matches with the protein curvature. As in eq. (5), the effective free energy for the CM model in terms of the bound fraction ρ is

$$f_{CM}(\rho) = \frac{\kappa a}{2}(2H)^2 + \frac{\bar{\kappa} a}{2}(2H - C_p)^2 \rho - \mu\rho + k_B T \left[\rho \log(\rho) + (1-\rho)\log(1-\rho) \right]. \tag{10}$$

For simplicity, we assume that $\kappa = \bar{\kappa}$ in the rest of the discussion. The equilibrium-bound fraction obtained after minimising the effective free energy with respect to ρ is

$$\rho_{eq} = \frac{1}{1 + e^{-\beta[\mu - \frac{\kappa a}{2}(2H - C_p)^2]}}. \tag{11}$$

Here again, the binding assumes the form of a shifted Langmuir isotherm. However, the effective binding affinity is different from that obtained for the SC model. For the CM model, the effective binding affinity takes the form

$$\mu' = \mu - \frac{\kappa a}{2}(2H - C_p)^2. \tag{12}$$

Here, the effective binding affinity is quadratic in the vesicle curvature, with an additional term $-2\kappa H^2 a$. This is unlike the SC model, where the dependence on curvature is linear.

For large vesicle radius (small H), we see no difference in the adsorption isotherm obtained with the two models (see figures 2a and 2c). The additional quadratic term in the effective binding affinity of CM model becomes relevant when the vesicle size is small (large H). Consequently, the curvature sensing curves predicted using the two models differ significantly as seen in figures 2b and 2d. While the SC model predicts a monotonic inverse relation between the protein-bound fraction and the vesicle radius, the CM model predicts a non-monotonic dependence. As the additional term is negligible at small vesicle curvatures ($H \ll C_p$), the predictions from the two models are similar for larger vesicles.

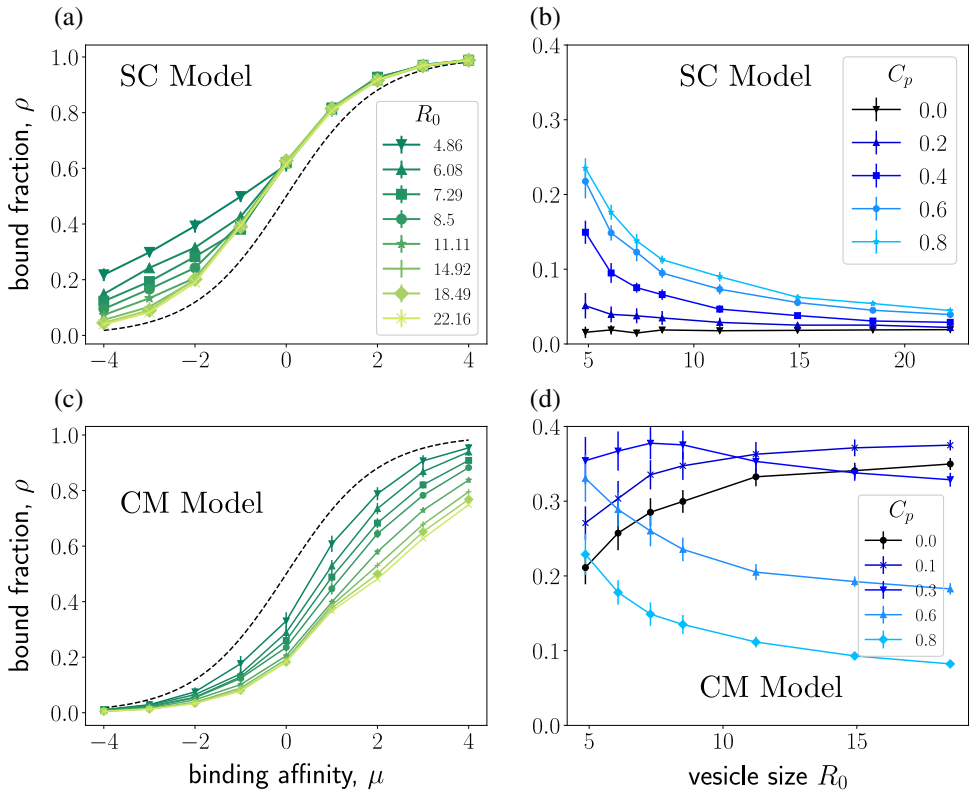

Figure 3. Analysis of protein binding on a deformable sphere modelled using the SC model and the CM model. Adsorption isotherms for vesicles of various sizes at $C_p = 0.6$ for (**a**) SC model and (**c**) CM model. Curvature-sensing curves for the SC model for different protein SC (**b**) at $\mu = -4$ for the SC model and (**d**) at $\mu = 0$ for the CM model.

One can ask the question – what is the size of the vesicle that shows maximum protein binding for proteins with fixed C_p at a given concentration (μ)? We see that for the SC model, the protein-bound fraction is maximum as $H \to \infty$ or in other words, for the smallest vesicle. On the other hand, the CM model predicts that the maximum binding is when the vesicle radius is C_p^{-1}, i.e. $H = C_p/2$. Essentially, the observed difference between the two models can be attributed to the fact that, in the CM model, a bound protein, in addition to inducing curvature, also adds to the membrane stiffness.

The analysis presented above is restricted to vesicles of fixed size and shape or in other words, the shape of the vesicle is assumed to not change on protein binding. The curvature generation by proteins is completely neglected because analytical minimisation of the free energy is complicated when we allow both the local mean curvature (H) and the protein-bound state (ϕ) to vary. Therefore, in the subsequent section, we use computer simulations to perform this minimisation where both curvature sensing and curvature generation by proteins are accounted for.

3. Curvature sensing and generation

We employed dynamic triangulation Monte Carlo (DTMC) simulations with protein binding, in the grand canonical ensemble, as described in ref. [27]. At any instant of the simulation, vesicles are represented by a triangulated surface, whereas proteins are represented by an occupation number defined at the vertices on the triangulated surface. The simulations are carried out using both the SC and CM models.

The adsorption isotherm obtained using the SC model is shown in figure 3a. At low μ, we see that the protein-bound fraction depends on the vesicle size at a fixed binding affinity. This is referred to as the curvature-sensing regime. At high values of μ, the protein binding fraction is independent of vesicle size. This is the curvature generation regime [27]. The adsorption curve for the CM model with $\bar{\kappa} = 10$ is shown in figure 3c. Although the adsorption isotherm appears to be Langmuir-like at small binding affinities, it significantly deviates from the Langmuir behaviour at higher μ values. For the SC model, curvature sensing happens at low binding affinity, whereas for the CM model, curvature sensing is more at higher binding affinities.

Curvature sensing is quantitatively measured using the equilibrium-bound fraction of proteins for different vesicle sizes at the same binding affinity. Curvature-sensing curve, from the SC model, monotonically increases with decreasing radius (see figure 3b), which is qualitatively similar to the predictions with non-deforming vesicles. At $C_p = 0$, the bound fraction is independent of the vesicle radius, i.e. there is no curvature sensing. For non-zero C_p, the bound fraction is maximum in the limit of zero radius. On the other hand, in the curvature-sensing curve for the CM model, shown in figure 3d, proteins with $C_p = 0.0$ is also coupled to the membrane curvature and senses it with more binding on larger vesicles. The simulation results show that, for $C_p \neq 0.0$, protein binding is maximum at a finite non-zero vesicle radius. When $C_p = 0.3$, there is a clear maximum at $R_0 \approx 7.0$. We expect that such maxima exist for other non-zero C_p values. However, they fall outside the range of vesicle radius studied in our simulations. Here again, the curvature-sensing curves are qualitatively similar to the curves obtained using the analytical model.

4. Concluding remarks

The main differences in results from the two models can be summarised as follows:

- SC model has a monotonic curvature-sensing behaviour, while the CM model has a non-monotonic sensing curve.
- The SC model has a curvature-sensing regime at low μ and a curvature-generation regime at high μ, whereas the CM model shows curvature sensing for all μ values explored here.
- The $C_p = 0$ case does not sense curvature in the SC model, while in the CM model, proteins show sensing behaviour at all C_p values.

The curvature-sensing behaviour is observed when the membrane is stiff. In the case of deformable vesicles, the binding of proteins leads to a softening of the membrane in both SC and CM models. In the CM model, there is also a term that rescales the effective bending modulus of the membrane with protein binding (see eq. (9)). Thus, the softening is significantly higher for the SC model than for the CM model. Consequently, for the same μ, protein binding is always higher for the SC model than for the CM model. At high μ in the SC model, the membrane is soft enough to conform to any protein curvature and hence we do not see curvature sensitivity. On the other hand, for the CM model, the membrane does not become soft enough to allow curvature generation even at high μ.

In the SC model, the coupling between protein density and membrane elasticity is only through the parameter C_p (refer eq. (3)), which serves as the source for curvature generation and sensing. At low C_p values, curvature sensing and generation is weak due to the weak coupling. Such a model is probably adequate for peripheral proteins that generate curvature through the hydrophobic insertion mechanism, where the strength of the coupling and the curvature generated are directly related. In the CM model, on the other hand, the parameter C_p has two contributions to the membrane elasticity. As in SC model, here too C_p serves as the coupling strength between the membrane curvature and protein density. In addition, it couples the membrane stiffness to the protein concentration through the $\bar{\kappa}$ term in eq. (9). Experimentally, such a scenario arises when the dominant interaction with the membrane is coming from a laterally extended region on the protein, say a region of charge leading to electrostatic binding. A recent finite-element analysis of curvature generation on a 3D linear elastic membrane has proposed that electrostatic interaction is essential for curvature generation by BAR domains [29]. Thus, the CM model may be more appropriate to model peripheral proteins that generate curvature using the scaffolding and other mechanisms such as oligomerisation or steric repulsion or in modelling transmembrane proteins.

Acknowledgements

Sachin Krishnan thanks IIT Palakkad for their hospitality and computational resources. The authors thank Department of Biotechnology, Ministry of Science and Technology, Government of India for the financial support through Grant No. BT/PR8025/BRB/10/1023/2013.

References

[1] H T McMahon and J L Gallop, *Nature* **438**, 590 (2005)
[2] J Zimmerberg and M M Kozlov, *Nat. Rev. Mol. Cell Biol.* **7**, 9 (2006)
[3] I K Jarsch, F Daste and J L Gallop, *J. Cell Biol.* **214**, 375 (2016)
[4] P Bassereau, R Jin, T Baumgart, M Deserno, R Dimova, V A Frolov, P V Bashkirov, H Grubmüller, R Jahn and H J Risselada, *J. Phys. D* **51**, 343001 (2018)
[5] K Farsad and P De Camilli, *Curr. Opin. Cell Biol.* **15**, 372 (2003)
[6] G K Voeltz and W A Prinz, *Nat. Rev. Mol. Cell Biol.* **8**, 258 (2007)
[7] Y Shibata, J Hu, M M Kozlov and T A Rapoport, *Annu. Rev. Cell Dev. Biol.* **25**, 329 (2009)

[8] B J Peter, H M Kent, I G Mills, Y Vallis, P J G Butler, P R Evans and H T McMahon, *Science* **303**, 495 (2004)
[9] V K Bhatia, K L Madsen, P Y Bolinger, A Kunding, P Hedegård, U Gether and D Stamou, *EMBO J.* **28**, 3303 (2009)
[10] N S Hatzakis, V K Bhatia, J Larsen, K L Madsen, P Y Bolinger, A H Kunding, J Castillo, U Gether, P Hedegård and D Stamou, *Nat. Chem. Biol.* **5**, 835 (2009)
[11] B Antonny, *Annu. Rev. Biochem.* **80**, 101 (2011)
[12] V Wasnik, N S Wingreen and R Mukhopadhyay, *PLoS ONE* **10**, 1 (2015)
[13] R L Gill, J P Castaing, J Hsin, I S Tan, X Wang, K C Huang, F Tian and K S Ramamurthi, *Proc. Natl. Acad. Sci. USA* **112**, E1908 (2015)
[14] A Martyna, J Gómez-Llobregat, M Lindén and J S Rossman, *Biochem. J.* **55**, 3493 (2016)
[15] W Draper and J Liphardt, *Nat. Commun.* **8**, 14838 (2017)
[16] T Baumgart, B R Capraro, C Zhu and S L Das, *Annu. Rev. Phys. Chem.* **62**, 483 (2011)
[17] S Aimon, A Callan-Jones, A Berthaud, M Pinot, G E S Toombes and P Bassereau, *Dev. Cell* **28**, 212 (2014)
[18] K R Rosholm, N Leijnse, A Mantsiou, V Tkach, S L Pedersen, V F Wirth, L B Oddershede, K J Jenses, K L Martinez and N S Hatzakis, *Nat. Chem. Biol.* **13**, 724 (2017)
[19] C Zhu, S L Das and T Baumgart, *Biophys. J.* **102**, 1837 (2012)
[20] B Božič, S L Das and S Svetina, *Soft Matter* **11**, 2479 (2015)
[21] S Svetina, *Eur. Biophys. J.* **44**, 513 (2015)
[22] B Sorre, A Callan-Jones, J Manzi, B Goud, J Prost, P Bassereau and A Roux, *Proc. Natl. Acad. Sci. USA* **109**, 173 (2012)
[23] M Mally, B Božič, S V Hartman, U Klančnik, M Mur, S Svetina and J Derganc, *RSC Adv.* **7**, 36506 (2017)
[24] W Helfrich, *Z. Naturforsch. C* **28**, 693 (1973)
[25] V S Markin, *Biophys. J.* **36**, 1 (1981)
[26] S Leibler, *J. Phys.* **47**, 507 (1986)
[27] T V Sachin Krishnan, S L Das and P B Sunil Kumar, *Soft Matter* **15**, 201 (2019)
[28] C Prévost, H Zhao, J Manzi, E Lemichez, P Lappalainen, A Callan-Jones and P Bassereau, *Nat. Commun.* **6**, 8529 (2015)
[29] P Mahata and S L Das, *FEBS Lett.* **591**, 1333 (2017)